IEEE/ASME Transactions on Mechatronics, Early Access Version

Ultra-High Temperature (250 C) Bearingless Permanent Magnet Pump for Aggressive Fluids

P. Peralta,
T. Wellerdieck,
D. Steinert,
T. Nussbaumer,
J. W. Kolar

This article has been accepted for publication in a future issue of this journal, but has not been fully edited. Content may change prior to final publication. Citation information: DOI 10.1109/TMECH.2017.2729618, IEEE/ASME Transactions on Mechatronics

Ultra-High Temperature (250 °C) Bearingless Permanent Magnet Pump for Aggressive Fluids

Patricio Peralta[1], Tobias Wellerdieck[1], Daniel Steinert[2], Thomas Nussbaumer[2], and Johann W. Kolar[1]
[1]Power Electronic Systems Laboratory, ETH Zurich, Switzerland
[2]Levitronix GmbH, Zurich, Switzerland
peralta@lem.ee.ethz.ch

***Abstract*—Bearingless pumps have been established in applications that demand high purity and reliability. To expand their temperature operation range, careful machine design is critical. High operating temperatures generate mechanical stress upon the dissimilar materials of the motor such as potting, copper, iron, etc., shortening their lifetime. To guarantee faultless operation, precise knowledge about internal operating temperatures is required. A bearingless motor capable of pumping the highest fluid temperature (250 °C) to our knowledge is presented. Thermal and hydraulic performance are experimentally verified.**

***Index Terms*—Magnetic levitation, synchronous machines, temperature measurement.**

I. Introduction

A bearingless machine is an electric motor with integrated magnetic bearing. Both functions are combined into one iron circuit, enabling a compact design. The rotor is suspended by a magnetic field, enabling its contact-free levitation and encapsulation [1], [2], as shown in Fig. 1(a). The rotor is disc shaped, ensuring passive stability in three degrees of freedom thus simplifying bearing control schemes.

The purpose of the pump is to handle corrosive fluids at ultra-high temperatures up to 250 °C with long lifetime and high purity [3]. Conventional pumps incorporate seals and mechanical bearings, which either contaminate the fluid or need frequent replacement under harsh conditions. High purity bellow pumps can be used up to 210 °C, yet systematically apply high mechanical stress upon fluoropolymers to pump. To this date, only bearingless machines are capable of handling fluids at 250 °C with high purity, as shown in this letter.

High fluid temperature handling capability and the demand for high purity represent a challenge to the durability of the motor. Pump components expand with temperature, thereby stressing structural interfaces. Materials that offer the required high chemical resistance and purity present only moderate mechanical strength, which drops even further with temperature. To withstand these conditions, the motor and pump head are mechanically supported by a thermoplastic polymer, and the hydraulic encapsulation is made out of fluoropolymers, whereas the copper coils are coated by a polyimide enamel. The pump is ultimately potted using medium-hardness silicon-based material. All components are rated for 250 °C.

Bearing and drive performance also decrease with temperature, making robust control schemes a necessity. Therefore, knowledge of the operating conditions of the constituting parts is crucial for the construction of a reliable pump.

To investigate the thermal condition of the components, a Lumped Parameter Thermal Model (LPTM) was built. The fluid and motor losses compose the heating mechanisms of the pump. Heat is dissipated to the ambient air through the finned case, whose convection model is critical for the accuracy of the temperature model. This study is presented in Section II.

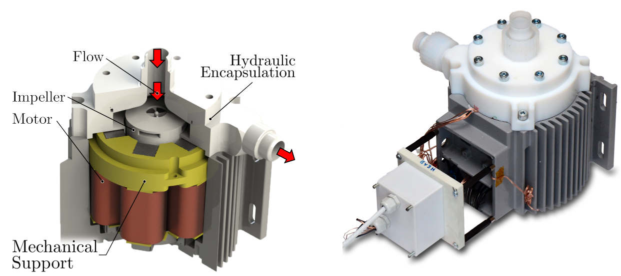

(a) (b)

Fig. 1: Schematic view (a) and photograph (b) of the bearingless ultra-high temperature pump.

The prototype of Fig. 1(b) was assembled, and has been tested over 20 times with fluid temperatures between 200 °C and 250 °C. Hydraulic tests were performed at 250 °C, enabling the verification of the LPTM and demonstrating that bearingless machines can be employed at such temperatures. The results are outlined in Section III.

II. Losses and Thermal Model

Figure 2(a) shows a sectional view of the pump along its LPTM. The most prominent heat source is the pumped fluid, modeled as a fixed temperature. At 250 °C, it heats the pump with roughly 200 W. The heat is initially conducted into the mechanical support and the iron tooth of the pump, where the heat is further transferred to the back iron, coils and potting. The latter has solid and ample contact to the finned casing, that ultimately dissipates the heat to the environment.

Heat transfer is modelled using thermal admittances, which are geometrically determined [4]. The admittance between the finned case and the environment was determined using approximative models [5] with posterior empirical correction.

Still, motor losses have a non negligible impact upon internal temperatures, accounting for 12 % of the total power heating up the machine. The latter are further separated into copper losses P_Ω and iron losses P_{Fe}, assessed by 3D finite element simulations, included in the LPTM of Fig. 2(a).

The N turns of each coil operate at different temperatures, hence with different resistances, contributing unevenly to the internal heating of the motor. The ohmic loss of each turn inside a coil is calculated, considering that excessive heating of windings can undermine the integrity of their insulation. This is critical for turns closer to the fluid and with no direct contact either to potting or iron. The sum of the winding losses over the total N turns results in the total copper losses P_Ω, equivalent to 11% of the total heating power.

This article has been accepted for publication in a future issue of this journal, but has not been fully edited. Content may change prior to final publication. Citation information: DOI 10.1109/TMECH.2017.2729618, IEEE/ASME Transactions on Mechatronics

Iron losses P_{Fe} are caused by the alternating sinusoidal magnetic flux density inside the stator. They are split into hysteresis $P_{\mathrm{Fe,Hy}}$ and eddy current losses $P_{\mathrm{Fe,Ed}}$ [6]. These losses are calculated with the Steinmetz equation, resulting in total iron losses P_{Fe}, comparable to 1% of total heat input.

The rotor consists of a rare earth permanent magnet, whose remanence flux magnetic density B_{r} drops with increasing temperature ϑ_{PM}. On the other hand, the field generated by the stator only depends on the current of the coils, as the B-H curve of iron remains unchanged with temperature, given that temperatures are far below its curie temperature of 700 °C.

The torque T and force F acting upon the rotor can be calculated as in [7], [8] resulting in $T, F \propto B_{\mathrm{r}}(\vartheta_{\mathrm{PM}})$. Given the temperature dependency of the rotor flux, it is deduced that to obtain a constant torque at increasing temperatures, the weakened flux of the rotor has to be compensated by a stronger flux coming from the stator, resulting in higher drive currents.

When pumping fluid at 250 °C, torque-current gain diminishes linearly up to 8% relative to its room temperature value. P_{Ω} will therefore rise quadratically with temperature, while $P_{\mathrm{Fe,Ed}}$ will lightly decrease given the decreasing currents in iron due to its increasing resistivity. $P_{\mathrm{Fe,Hy}}$ remains practically unaffected, thanks to the temperature-independent B-H curve of iron. All in all, the 86% motor efficiency at room temperature decreases to 81% when pumping fluids at 250 °C.

III. Results

A pump prototype is built, and mounted in a close-circuit test stand with 2" diameter tubing, where it pumps silica oil at regulated temperature. Pressure difference was measured with two pressure sensors at the inlet and outlet of the pump head, while the flow was measured with a high-temperature float-type flowmeter, followed by a manual valve. A schematic view of the test stand, as well as the achieved hydraulic operating points at 250 °C are shown in Fig. 2(b).

Five temperature probes were included inside the prototype, at various nodes of the LPTM from Fig. 1(b). Table I shows the measured and estimated temperatures.

The model estimates internal temperatures with acceptable accuracy. The calculated thermal admittance of the case was corrected in an enclosure smaller than the safety case of the hydraulic test stand. This procedure underestimated the admittance, thus overestimating case temperature. Coil surface temperature also showed discrepancy, since the temperature probe was inserted between the coil and a support piece, to avoid misplacement during motor assembly and potting. The piece partially blocks heat exchange from coil to potting, increasing temperature at the coil interface.

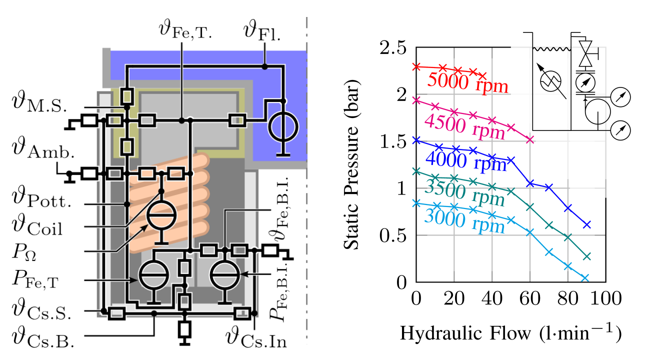

(a) (b)

Fig. 2: Cross sectional view of the pump showing the LPTM (a) and hydraulic specifications of the prototype, pumping silica oil at 250 °C, along with P&ID schematic of the hydraulic test stand (b).

TABLE I: Verification of the thermal model for 250 °C fluid temperatures, measured at a flow of 90 l·min^{-1} and at 3000 rpm.

Position	Symbol	Model	Measured (°C)	Error (%)
Oil	$\vartheta_{\mathrm{Fl.}}$	250		
Ambient	$\vartheta_{\mathrm{Amb.}}$	50		
Coil Surface	$\vartheta_{\mathrm{Coil}}$	87.9	97.1	−9.4
St. Back Iron	$\vartheta_{\mathrm{Fe,B.I.}}$	92.9	92.9	0.2
St. Iron Tooth	$\vartheta_{\mathrm{Fe,T.}}$	105.3	105	0.3
Mech. Supp.	$\vartheta_{\mathrm{M.S.}}$	161.8	150.5	5.5
Case	$\vartheta_{\mathrm{Cs.S.}}$	80.4	70	14.9

In absolute terms, Table I clearly shows how all measured points are practically 90 °C under the 250 °C component maximum ratings. These operating margins ensure long-lasting lifetimes. To this end, the pump has withstood more than 20 test cycles pumping between 200 °C and 250 °C, validating the correct material selection.

IV. Conclusion and Outlook

This letter outlines the latest advances in bearingless pumps, presenting experimental results with the highest fluid temperatures as of today with high purity standards. This shows how careful modeling and material selection enable the successful construction of a working prototype, whose hydraulic performance at 250 °C fluid temperature at various operating points was tested. The internal temperatures do not exceed material ratings, allowing the prototype to endure numerous high temperature tests and giving promising insight upon long lifetime operation capabilities.

The results prove that pumping aggressive fluids at high temperatures with high purity is only possible with bearingless motors, thereby expanding their range of applications.

V. Acknowledgement

This work was supported by the *Swiss Commission for Technology and Innovation CTI-KTI*.

References

[1] T. Schneeberger, T. Nussbaumer, and J. W. Kolar, "Magnetically levitated homopolar hollow-shaft motor," *IEEE/ASME Transactions on Mechatronics*, vol. 15, pp. 97–107, Feb 2010.

[2] X. Sun, L. Chen, and Z.Yang, "Overview of bearingless permanent-magnet synchronous motors," *Industrial Electronics, IEEE Transactions on*, vol. 60, no. 12, pp. 5528–5538, 2013.

[3] R. Schöb, "Centrifugal pumps without bearing or seals," *World Pumps*, vol. 430, no. 12, pp. 34–37, 2002.

[4] J. Pyrhonen, T. Jokinen, and V. Hrabovcova, *Design of Rotating Electrical Machines*. John Wiley & Sons, 2009.

[5] V.-G. V. und Chemieingenieurwesen, *VDI Heat Atlas*. Springer reference, Springer, 2010.

[6] C. Mi, G. Slemon, and R. Bonert, "Minimization of iron losses of permanent magnet synchronous machines," *Energy Conversion, IEEE Transactions on*, vol. 20, pp. 121–127, March 2005.

[7] B. Laptre, N. Takorabet, F. Meibody-Tabar, J. Fontchastagner, R. Lateb, and J. D. Silva, "New model of radial force determination in bearingless motor," *IEEE Transactions on Magnetics*, vol. 51, pp. 1–4, March 2015.

[8] T. Wellerdieck, T. Nussbaumer, and J. Kolar, "Angle-sensorless zero- and low-speed control of bearingless machines," *IEEE Transactions on Magnetics*, vol. PP, no. 99, pp. 1–1, 2016.